

Article

The Effects of Different Geological Conditions on Landslide-Triggering Rainfall Conditions in South Korea

Jae-Uk Lee ¹, Yong-Chan Cho ², Minseok Kim ³, Su-Jin Jang ⁴, Jongmyoung Lee ^{1,5} and Sukwoo Kim ^{6,*}

¹ Department of Forestry and Environmental Systems, Kangwon National University, Chuncheon 24341, Korea; rksk85234@kangwon.ac.kr (J.-U.L.); jml@foresti.co.kr (J.L.)

² Mineral Resources Division, Korea Institute of Geoscience and Mineral Resources, Daejeon 34132, Korea; choych@kigam.re.kr

³ Geologic Hazards Division, Korea Institute of Geoscience and Mineral Resources, Daejeon 34132, Korea; minseok_kim@kigam.re.kr

⁴ Institute of Forest Science, Kangwon National University, Chuncheon 24341, Korea; sujinjang@kangwon.ac.kr

⁵ Forest Information Corporation, Namyangju 12106, Korea

⁶ Division of Forest Science, Kangwon National University, Chuncheon 24341, Korea

* Correspondence: kimsw@kangwon.ac.kr; Tel.: +82-33-250-8311

Abstract: How landslide-triggering rainfall conditions vary with geology is unclear. The effects of three different geological conditions (gneiss, GN; granite, GR; sedimentary rock, SR) on variations in intensity–duration (I-D) conditions and rainfall characteristics responsible for initiating shallow landslides were examined using data from 476 landslides in South Korea from 1963 to 2018 and detailed statistical analyses. Results from quantile regression and one-way analysis of variance analyses clearly showed that impermeable SR slopes result in smaller critical rainfall than permeable GN and GR slopes do, indicating a relatively high occurrence exceedance probability and susceptibility to landslides in SR slope. These findings suggest that geological conditions, particularly the relatively high susceptibility of SR slopes, should be considered when establishing rainfall information-based landslide warning criteria for South Korea. Our findings can contribute to the assessment of landslide susceptibility and probability based on geological conditions; however, they should be further investigated through in situ observations.

Keywords: statistical analysis; landslide-triggering rainfall; geological condition; South Korea



Citation: Lee, J.-U.; Cho, Y.-C.; Kim, M.; Jang, S.-J.; Lee, J.; Kim, S. The Effects of Different Geological Conditions on Landslide-Triggering Rainfall Conditions in South Korea. *Water* **2022**, *14*, 2051. <https://doi.org/10.3390/w14132051>

Academic Editors: Chien-yuan Chen and Renato Morbidelli

Received: 1 May 2022

Accepted: 23 June 2022

Published: 27 June 2022

Publisher's Note: MDPI stays neutral with regard to jurisdictional claims in published maps and institutional affiliations.



Copyright: © 2022 by the authors. Licensee MDPI, Basel, Switzerland. This article is an open access article distributed under the terms and conditions of the Creative Commons Attribution (CC BY) license (<https://creativecommons.org/licenses/by/4.0/>).

1. Introduction

The occurrence of landslides is a dominant factor that contributes to the erosion and deformation of the Earth's surface. Landslides are the most common geological hazard in many mountainous terrains. The initiation of landslides is governed by various natural factors, such as meteorology, geology, topography, and vegetation cover. Of those factors, rainfall and geological conditions are possibly the most important external and internal factors, respectively, in relation to the initiation of landslides [1–7].

The association between rainfall intensity and duration (I-D) has been commonly used to assess and predict the possibility of landslide occurrence on global [8,9] and regional scales, including for the Piedmont region in Italy [10], central and southern Europe [11], Wayanad district in India [12], southwestern Colorado and southern California in the United States of America [13], Japan [14,15], the Tuscany region in Italy [16], Taiwan [17], and South Korea [18]. The regional thresholds of landslide-triggering rainfall have often been compared with those proposed for other regions [10,11,13,15,17,18], even though they reflect the influence of various factors, such as the meteorological, lithological, and topographical conditions in a specific region. It has also been reported that some regional I-D thresholds vary depending on antecedent rainfall conditions [18,19], clear-cutting [20], permeability of sedimentary rocks (i.e., mudstone and sandstone [14]), and types of mass

movements [17]. However, how the geological conditions affect I-D thresholds and conditions of landslide-triggering rainfall remains poorly understood.

Rainfall conditions that trigger landslides can vary regionally depending upon geological conditions or lithology [14,21,22]; nevertheless, rainfall is well known as the primary trigger of shallow landslides [10,17,18,23,24]. Matsushi and Matsukura [14] found that the critical intensities of landslide-triggering rainfall were higher for permeable sandstone slopes than those for impermeable mudstone slopes. Moreover, lithological or geological conditions, including physical and weathering characteristics [3,25,26], can control the triggering mechanism, type, and pattern of landslides. Kim and Song [5] noted that the shape and size of a landslide are related to geological conditions and, in particular, the size and depth of landslides are smaller and shallower in sedimentary rock terrain than those in gneiss and granite terrains in South Korea. Igwe [6] found that landslides in south-east Nigeria were characterized by slumps and short-runout slides with low volumes in sedimentary terrain, whereas landslides with complex transitional and rotational movements with long runout distances occurred in metamorphic terrain. Bartelletti et al. [7] reported that bedrock lithology seems to be an important factor that influences the localization of shallow landslide source areas in the northern Apennines of Italy. Kim et al. [18] noted the influence of geological conditions, which can cause differences in rainfall infiltration rates, on the initiation of landslides. Therefore, understanding the geological characteristics of a specific region and the influence of those characteristics on the probability of landslide occurrence provides useful insights into the landslide susceptibility of the region.

The effect of geological conditions on landslides may be related to the mechanical properties of the soil present in the slope and originating from parent rock. The physical and mechanical properties of soils vary depending on geological conditions because they are the results of physical and chemical weathering of bedrock [2,5]. Granite soil, which consists of coarse-grained materials, has a larger pore size than soil derived from sedimentary rocks, such as mudstone and shale, which consists of very fine-grained materials, i.e., silts and clays [2]. Soil properties are also affected by the composition of minerals present, which depend on the geological conditions of the site [27,28]. The content and geochemical characteristics of the minerals constituting the soils are important factors in landslide susceptibility and size [28]. Consequently, hillslope erodibility may vary in terms of susceptibility to rainfall-triggered landslides, depending on the mechanical and hydrological properties of the soil that originated from the parent rock [5,14]. However, the quantitative relationship between slope soil, slope hydrology, and critical rainfall remains unclear [14]. Therefore, the investigation of these relationships can help in evaluating landslide activity under different geological conditions.

In South Korea, shallow landslides frequently occur in the surficial layer above bedrock in diverse geological settings during the summer rainy season from June to September [18,21,29], suggesting that understanding the influence of different geological conditions and rainfall on landslides is critically important in the establishment of a landslide warning system and can provide a good opportunity to explore the influence of different geological conditions. This study is aimed at (1) investigating the differences and variations in I-D conditions and rainfall characteristics for three major geological conditions (gneiss, GN; granite, GR; sedimentary rock, SR) using data from 476 shallow landslides in South Korea and (2) assessing the influence of these geological conditions on rainfall-triggered landslides in terms of occurrence exceedance probability and landslide susceptibility.

2. Materials and Methods

2.1. Geographical Settings of South Korea

South Korea, which is located in the mid-latitude zone of the Northern Hemisphere (33–39° N), is affected by the East Asian monsoon. The mean annual temperature and mean annual precipitation vary regionally from 6.6 to 16.6 °C and from 825.6 to 2007.3 mm, respectively [30]. More than 50% of the annual precipitation occurs during heavy rainfall

in the summer season, i.e., June to September [18,29]. This is consistent with the monthly distribution of landslide occurrences, indicating that rainfall is the primary triggering factor in landslides [18].

Approximately 64% of the land in South Korea is mountainous terrain, 62.5% of which has steep slopes ($>30^\circ$) [31]. Because of the high population density of the country, the land around mountainous terrain has traditionally been inhabited, and, recently, the topography of mountainous terrain has been altered in response to the expansion of urban areas. Consequently, the inhabitants of such areas are potentially at risk of losing their lives to landslide hazards caused by rainfall [32].

In terms of the geology of Korea, metamorphic, igneous, and sedimentary rocks comprise 42.6%, 34.8%, and 22.6% of the entire land area [33], respectively, with high lithologic diversity dating from the Precambrian to the Cenozoic periods [34] (Figure 1). Gneiss and granite are the major rock types accounting for approximately 65% of the metamorphic and igneous rock terrains, respectively. As a result, these rock types, along with sedimentary rock, have received considerable attention in research on the association of landslide occurrence with geological conditions in Korea [2,21,28,35].

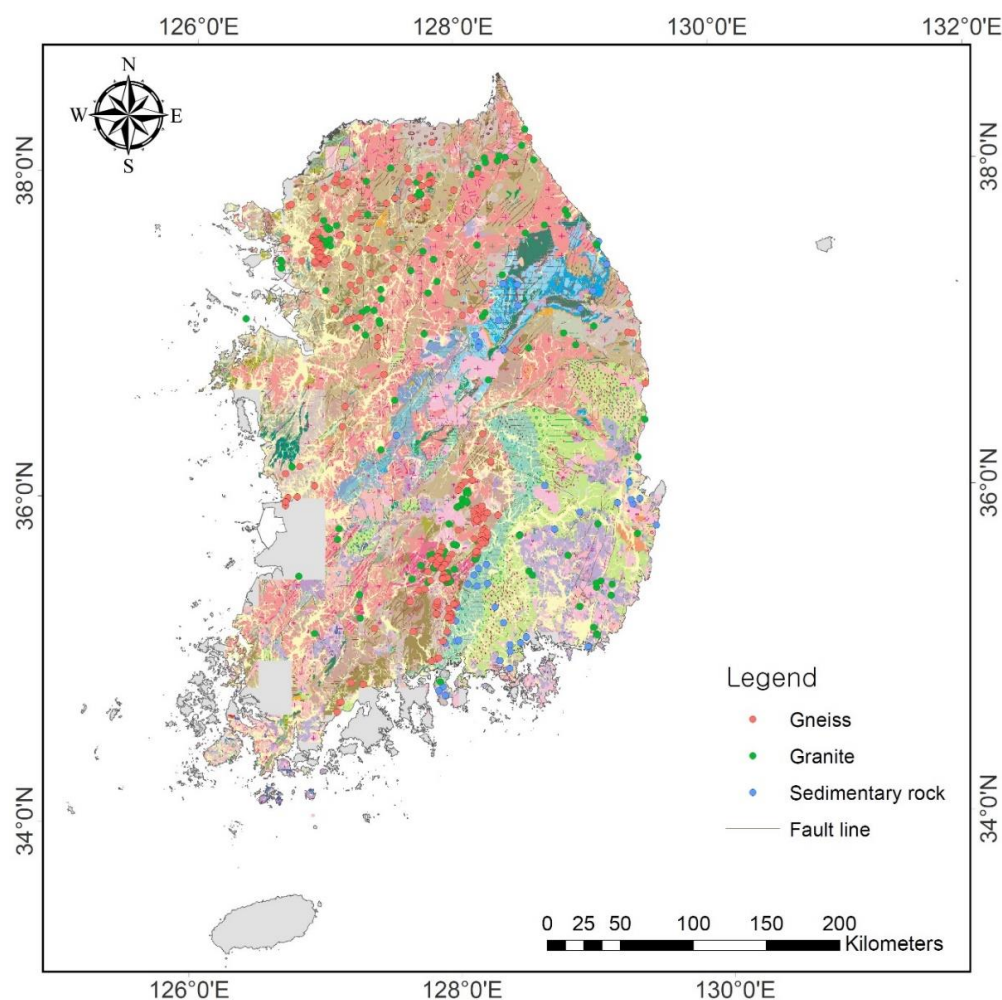


Figure 1. Locations of 476 rainfall-triggered shallow landslides in South Korea on a 1:250,000-scale geological map. The areas shaded in gray depict the area of a digital geological map that is currently being built.

2.2. Data Collection

2.2.1. Landslide Data

The size of the dataset may be a critical issue when determining the validity and reliability of empirical analysis based on the measurement or observation of a target

phenomenon. Although landslides frequently occur during summer in South Korea, the available data on the occurrence times and locations of landslides is limited except for recent landslides in urban areas. Prior to the present study, Kim et al. [18] constructed a dataset which contained spatiotemporal information (i.e., location and time of occurrence) on 613 rainfall-triggered shallow landslides that occurred from 1963 to 2018 in South Korea and subsequently established I-D thresholds by analyzing the corresponding hourly rainfall data. This information was derived from research articles, archives of major national and local newspapers, and scientific reports. Newspaper articles provide information on the time and location of landslides based on interviews with local residents, and, therefore, have been used to collect landslide occurrence information in previous studies [16,18,22].

Using the same dataset used by Kim et al. [18], we investigated the geological conditions corresponding to the locations of 613 shallow landslides. A geographic information system was used to map the geographic coordinates of the locations of the landslides (558 specific sites and 55 unspecified mountainous hillslopes in specific villages) at a 1:250,000 scale onto a digital geological map developed by the Korea Institute of Geoscience and Mineral Resources (KIGAM). The geological conditions of the landslide locations were then analyzed. The geological conditions of the sites were classified into three major categories, namely, igneous, metamorphic, and sedimentary rocks, based on the geotechnical properties (i.e., the physical and weathering characteristics) of the rocks in the area. Igneous rocks were subcategorized into granite (granite and syenite), diorite (diorite, amphibolite, and gabbro), or volcanic rock (andesite and tuff) depending on the prevalence and chemical composition of the rocks. Metamorphic rocks were subcategorized into gneiss (granite gneiss, banded gneiss, augen gneiss, and schist) and phyllite according to the metamorphic grade, as the names of the rocks and stratigraphy were mixed on the geological map. Sedimentary rocks include Cretaceous sedimentary rocks, Tertiary sedimentary rocks (mudstones), and limestone. Of the 613 landslides analyzed, 476 occurred on GN, GR, and SR terrains, which are the three major geological conditions associated with frequent occurrence of landslides [2,21,28], and these 476 landslides (Figure 1) were selected for analysis. GN and GR account for the majority of metamorphic and igneous rocks, respectively, in South Korea [36]. The pie chart in Figure 2 shows the distribution of the geological conditions of the 476 landslides. This distribution is quite similar to the distribution of geological conditions on the Korean Peninsula as a whole.

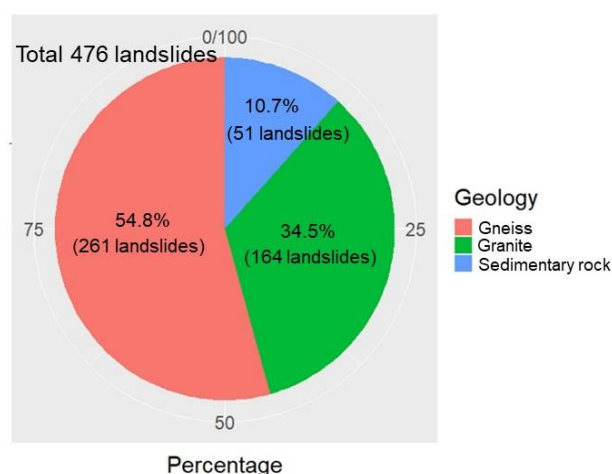


Figure 2. Distribution of the geological conditions of the 476 selected landslides.

2.2.2. Rainfall Data

Hourly rainfall data corresponding to the rainfall events that triggered the landslides were obtained from the meteorological stations closest to each of the landslide locations. Stations with no missing values that were situated within a maximum distance of 13 km (the average distance between meteorological stations in South Korea [36]) from each

landslide location were selected. The original hourly rainfall data were obtained from a total of 184 meteorological stations across the country: 72 stations affiliated to the Korea Meteorological Administration (KMA), one station affiliated to the Korea Aviation Meteorological Office, two stations affiliated to the Korea Forest Service, and 109 stations affiliated to the Korea Ministry of Environment, including the Korea Water Resource Corporation. The average distance between the locations of landslides and meteorological stations was 5.0 ± 2.7 km (average \pm standard deviation) in GN terrains, 4.5 ± 2.6 km in GR terrains, and 4.8 ± 2.6 km in SR terrains. In this study, interpolation methods could not be applied to reproduce the hourly rainfall data because of the non-uniform distribution of the meteorological stations, given the mountain terrain in many locations [37], and the lack of continuous hourly rainfall data at many adjacent weather stations, particularly for landslides that occurred from the 1960s to the 1980s.

The 30-year average annual precipitation, which was defined as a climatological (standard) normal [38], was used as the representative mean annual precipitation (MAP) of a given region to rescale the mean rainfall intensity related to landslide occurrences. These data were collected from the 51 closest KMA meteorological stations possessing long-term observation data [30,39,40].

2.3. Rainfall Data Analysis

2.3.1. Definition of Landslide-Triggering Rainfall

When analyzing the rainfall characteristics that trigger landslides, the most important issue is determining the time when a rainfall event began [10,41–43]. According to Rosi et al. [41], reasonable criteria must be established to exclude the possibility of subjective intervention when defining the starting point at which rainfall thresholds responsible for the initiation of landslides are identified. However, this is difficult to achieve because multiple rainfall patterns coexist [41] and landslides are triggered by various types of heavy rain in South Korea [29]. Therefore, we determined the start of the landslide-triggering rainfall event for each landslide by delimiting it by at least 24 h of no rainfall (Figure 3), as has been conducted in several studies [15,44–46]. Using this method, we defined an independent landslide-triggering rainfall event as a series of events from the beginning of the rainfall to the landslide occurrence. We then analyzed the following rainfall parameters: the event cumulative rainfall (ECR, mm), mean intensity (I , mm h^{-1}), 1-h intensity at the occurrence instant (I_{oi} , mm h^{-1}), duration (D , h), and elapsed time (T_e , h) (Figure 3).

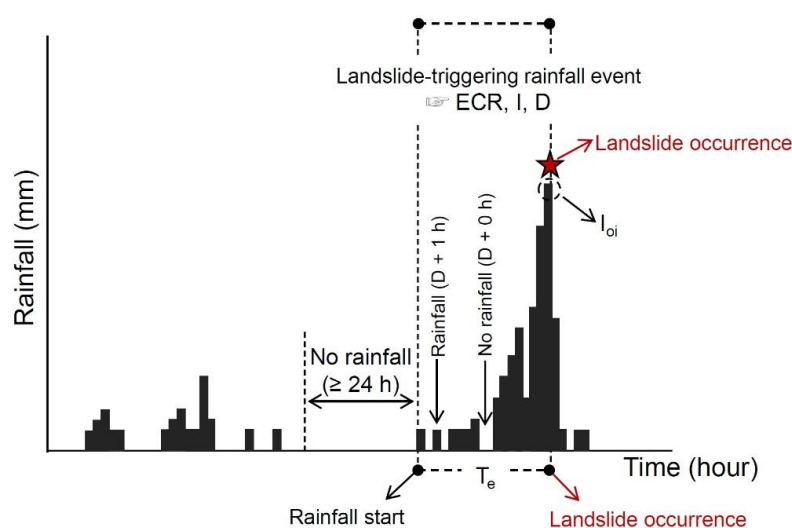


Figure 3. Definition of landslide-triggering rainfall event and the parameters used in the present study. Abbreviations: I , mean intensity; D , duration; ECR, event cumulative rainfall; I_{oi} , 1-h intensity at the occurrence instant; T_e , elapsed time.

2.3.2. Intensity–Duration Condition

The rainfall thresholds resulting in the initiation of landslides were expressed as a combination of intensity (I) and duration (D) according to the power law model proposed by Caine [8], as follows:

$$I = \alpha D^{-\beta}, \quad (1)$$

where α and β are regression coefficients. I-D plots are typically drawn with logarithmic scales for both the x (D) and y (I) axes, and the regression line of the minimum level is regarded as the rainfall threshold that is most likely to trigger a landslide [8,11,15,18].

To investigate the I-D relationship in each geological condition, a quantile regression method was applied to determine the landslide-triggering rainfall threshold using the R statistical software package (ver. 3.4.3) [47], as performed in several previous studies [15,18,29]. Quantile regression analysis was performed at the 2nd, 50th, and 90th percentile levels, according to the methods propounded by Guzzetti et al. [11] and Saito et al. [15]. The regression lines corresponding to the three percentiles were defined as the minimum (i.e., threshold), moderate (general trend), and maximum levels, respectively, and were then compared at each percentile level, according to the geological conditions. Additionally, the direct comparison between the regional I-D thresholds is limited because of the climatological and meteorological variations observed in different regions [48]. Therefore, the I-D thresholds were normalized by dividing I by MAP (I_{MAP}) to eliminate the effects of variations in regional meteorology and enable the comparison of the three geological conditions.

2.3.3. Statistical Differences in Rainfall Characteristics

Among the three geological conditions, differences in the rainfall parameters (i.e., ECR, I, I_{MAP} , I_{oi} , MAP, and D/T_e , D) were analyzed using nonparametric one-way analysis of variance (ANOVA) (i.e., a Kruskal–Wallis test) after testing for normality. When the results of a one-way ANOVA were significant, a Mann–Whitney post hoc test was used to explore the specific differences between groups. The significance level was set to $\alpha = 0.05$ (i.e., $p < 0.05$). All the statistical analyses were performed using the SPSS statistical software (ver. 26, Chicago, IL, USA).

3. Results

3.1. Rainfall Thresholds for Different Geological Conditions

The scatter plots in Figure 4a,b show the rainfall I-D and I_{MAP} -D conditions that have triggered shallow landslides in GN (261 red dots), GR (164 green dots), and SR (51 blue dots) terrains, on double logarithmic scales. In the plots, the dotted, dashed, and solid lines denote the regression lines of the 2nd, 50th, and 90th percentiles, respectively, for GN (red lines), GR (green lines), and SR (blue lines) terrains. The power-law I-D and I_{MAP} -D equations corresponding to the regression lines of the 2nd, 50th, and 90th percentiles for each geological condition are presented in Table 1.

The rainfall durations for GN, GR, and SR terrains ranged from 4 to 72 h, 6 to 84 h, and 6 to 54 h, respectively, revealing a slightly narrower range for SR terrains. In the I-D plot (Figure 4a), the regression line for SR is lower than those for GN and GR after $D = 16$ h for the 2nd percentile (i.e., threshold) and is consistently lower than those for GN and GR at the 50th and 90th percentiles, showing that such differences increased with increasing percentile. In the I_{MAP} -D plot (Figure 4b), in which the influence of MAP is eliminated, the regression line for SR is consistently lower than those for GN and GR at $D = 10$ h for the 2nd percentile, and is similar to the I-D relationships for the 50th and 90th percentiles. The I-D and I_{MAP} -D plots also show that the threshold and two regression lines for SR are lower than those for the entire area of South Korea, which is characterized by an intermediate trend between those for GN and GR. These results demonstrate that hillslopes in SR terrains are more susceptible to landslides than those in GN and GR terrains, particularly under relatively high rainfall intensity conditions. The results also suggest that the I-D conditions

and thresholds for possible initiation of landslides, and thus the probability of landslide occurrence for a given rainfall amount vary depending on a region’s geological conditions.

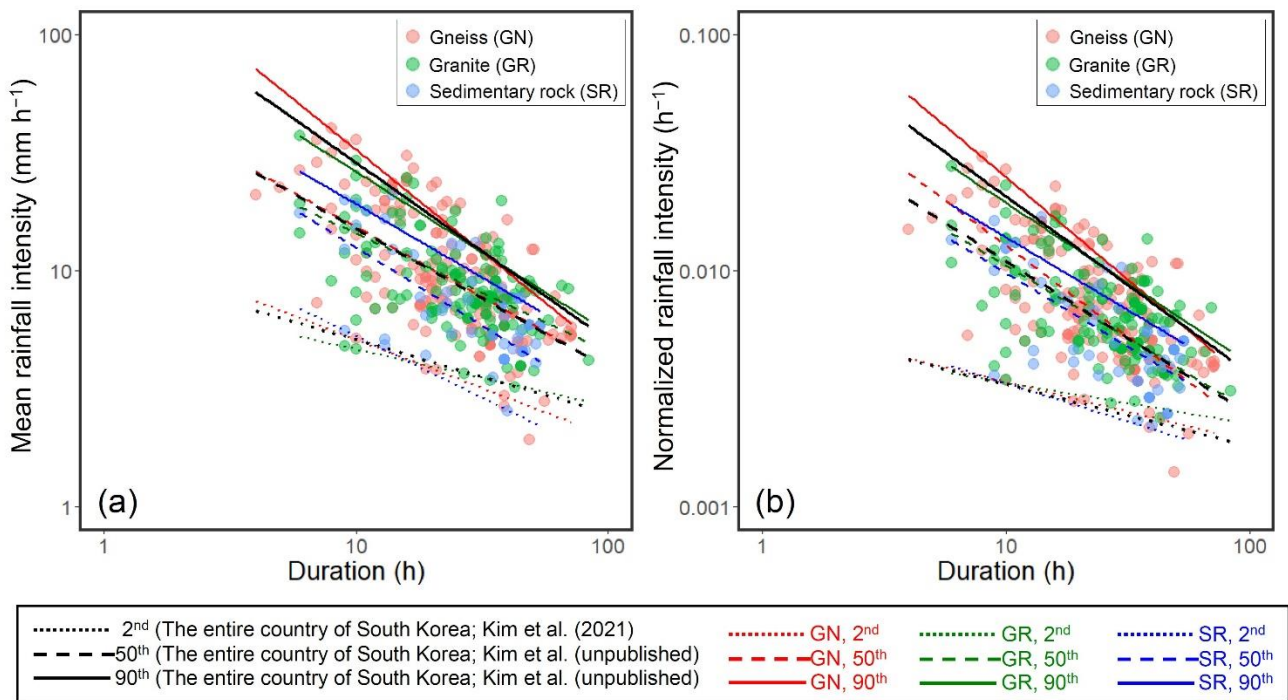


Figure 4. Rainfall I-D (a) and I_{MAP-D} (b) plots that triggered shallow landslides for different geological conditions in South Korea.

Table 1. The rainfall I-D (a) and I_{MAP-D} (b) equations derived from the quantile regression analyses for different geological conditions.

Geological Condition	No. of Landslides	Equation			Range
		Type	2nd Percentile	50th Percentile	
GN ¹	261	I-D	$I = 13.13 \times D^{-0.41}$	$I = 59.48 \times D^{-0.59}$	$I = 234.59 \times D^{-0.86}$
		I_{MAP-D}	$I = 0.006 \times D^{-0.250}$	$I = 0.075 \times D^{-0.769}$	$I = 0.183 \times D^{-0.867}$
GR	164	I-D	$I = 8.06 \times D^{-0.24}$	$I = 45.38 \times D^{-0.50}$	$I = 125.38 \times D^{-0.68}$
		I_{MAP-D}	$I = 0.005 \times D^{-0.174}$	$I = 0.043 \times D^{-0.612}$	$I = 0.093 \times D^{-0.681}$
SR	51	I-D	$I = 17.49 \times D^{-0.52}$	$I = 57.15 \times D^{-0.66}$	$I = 79.67 \times D^{-0.62}$
		I_{MAP-D}	$I = 0.007 \times D^{-0.322}$	$I = 0.041 \times D^{-0.623}$	$I = 0.057 \times D^{-0.615}$

¹ GN: gneiss, GR: granite, and SR: sedimentary rock.

Table 2 lists the values of ECR calculated using the I-D equations (Table 1) for overlapping ranges of $D = 6-54$ h for each percentile and the three geological conditions. According to the I-D threshold equations for the 2nd percentile, the ECR that is likely to trigger landslides is the smallest for SR terrains, except at $D = 6$ h. For the 50th and 90th percentiles, the ECR is also the smallest for the SR terrains. The difference between GN and GR was slight, whereas the difference between these two rocks and SR was relatively large. On average, the ECR is 1.1–1.2 (+8.0 mm and +18.6 mm in amount), 1.3–1.4 (+53.5 mm and +61.6 mm), and 1.3 times (+93.0 mm and +77.9 mm) larger for the GN and GR terrains than for the SR terrains for a given rainfall duration for the 2nd, 50th, and 90th percentiles, respectively, showing that the higher the percentile is, the greater the difference in the mean ECR is.

Table 2. Comparison of ECR calculated from I-D equations for each percentile of different geological conditions.

Percentile	D (h)	Calculated ECR (mm)		
		GN ¹	GR	SR
2nd	6	37.8 (0.9) ²	31.5 (0.8)	41.3 (1.0)
	30	97.7 (1.1)	106.9 (1.2)	89.5 (1.0)
	54	138.2 (1.2)	167.1 (1.4)	118.7 (1.0)
	Mean	91.2 (1.1)	101.8 (1.2)	83.2 (1.0)
50th	6	124.0 (1.2)	111.2 (1.1)	105.1 (1.0)
	30	239.9 (1.3)	248.6 (1.4)	181.7 (1.0)
	54	305.2 (1.4)	333.5 (1.5)	221.8 (1.0)
	Mean	223.0 (1.3)	231.1 (1.4)	169.5 (1.0)
90th	6	301.5 (1.9)	222.5 (1.4)	157.4 (1.0)
	30	377.7 (1.3)	372.3 (1.3)	290.1 (1.0)
	54	410.1 (1.1)	449.4 (1.2)	362.7 (1.0)
	Mean	363.1 (1.3)	348.0 (1.3)	270.1 (1.0)

¹ GN: gneiss, GR: granite, and SR: sedimentary rock. ² The values in parentheses indicate the ratio of a given ECR to that of SR at each rainfall duration D.

3.2. Comparison of Rainfall Characteristics

Figure 5 shows boxplots of the duration (a) and ratio of duration to elapsed time (b), which are time parameters of landslide-triggering rainfalls for the three geological conditions. The ratio of duration to elapsed time (D/T_e) can be regarded as a measure of rainfall concentration. The mean values of D (h) were 29.6 (range: 4–72), 29.2 (range: 6–84), and 32.7 (range: 6–54) (h) for the GN, GR, and SR terrains, respectively, showing that there was no statistical difference among the groups ($p = 0.074$; Figure 5a). However, there was a significant difference in the mean values of D/T_e among the groups ($p = 0.015$; Figure 5b). In other words, the mean values for GN (0.74, $p = 0.051$) and GR (0.75, $p = 0.004$) were marginally and significantly higher, respectively, than the value for SR (0.66), and SR exhibited the lowest value. There was no significant difference between the values for the GN and GR groups ($p = 0.111$).

Figure 6 shows the boxplots of ECR (a), I (b), I_{oi} (c), and I_{MAP} (d), which are associated with the size parameters of landslide-triggering rainfall for each geological condition. The mean values of ECR (mm), I (mm h^{-1}), I_{oi} (mm h^{-1}), and I_{MAP} (h^{-1}) were as follows: 253.1 (range: 51.0–655.0), 10.3 (range: 1.9–40.1), 34.7 (range: 0.0–103.0), and 0.008 (range: 0.001–0.030), respectively, for GN; 241.6 (range: 48–752), 9.5 (range: 3.2–37.1), 30.7 (range: 0.0–131.5) and 0.007 (range: 0.002–0.028), respectively, for GR; and 200.6 (range: 47.0–338.0), 7.4 (range: 2.6–19.9), 22.9 (range: 0.0–83.0), and 0.005 (range: 0.002–0.016), respectively, for SR showing that the mean values of all parameters were the lowest for SR. The ANOVA results show significant differences in the mean values of all parameters among the groups ($p < 0.05$ for all parameters). The mean values for GN and GR were significantly different from those for SR at the given significance levels for all parameters ($p < 0.05$). However, except for I_{oi} ($p = 0.022$), no notable differences were detected between the GN and GR groups ($p > 0.05$).

The above results suggest that the rainfall intensities, concentrations, and hence, the amounts that are likely to cause landslides are significantly lower for SR terrains than for GN and GR terrains, as shown in Figure 4 and Table 2.

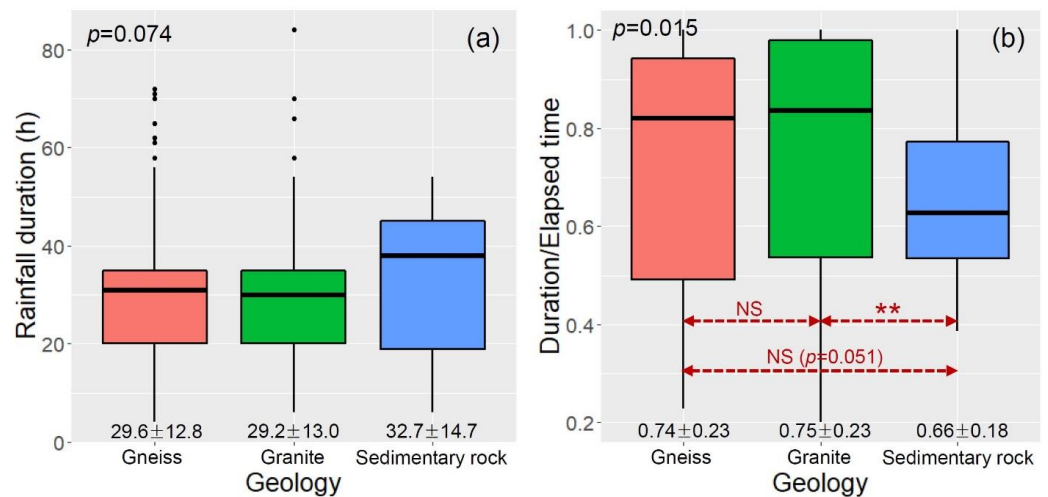


Figure 5. Boxplots of D (a) and D/T_e (b) for each geological condition. (** $p < 0.01$ and NS = not significant from one-way ANOVA analysis with post hoc test). The black dots represent outliers and values below each box indicate the mean \pm standard deviation.

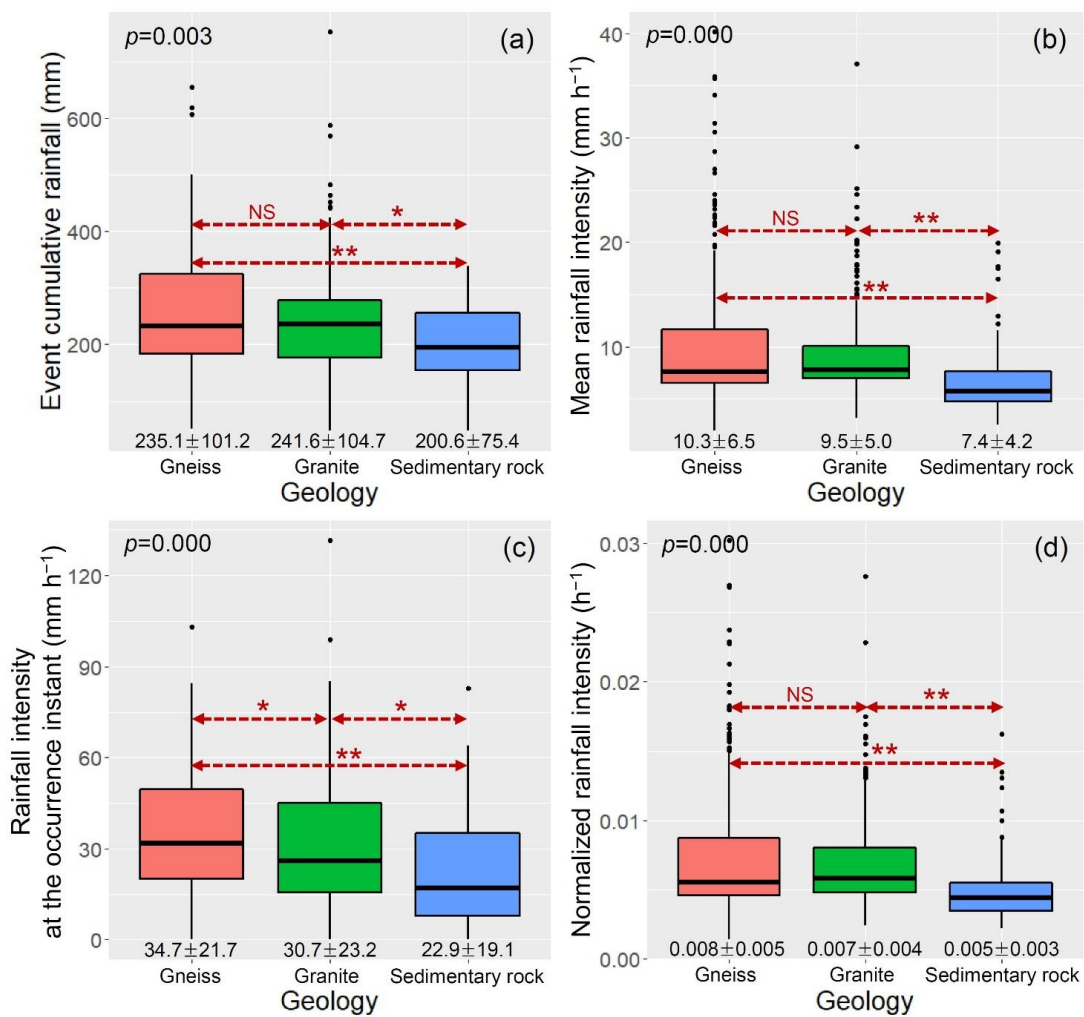


Figure 6. Boxplots of ECR (a), I (b), I_{oi} (c), and I_{MAP} (d) for each geological condition (* $p < 0.05$, ** $p < 0.01$, and NS = not significant from one-way ANOVA analysis with post hoc test). The black dots represent outliers and values below each box indicate the mean \pm standard deviation.

4. Discussion

The differences in regional I-D thresholds have often been considered as the result of landform adjustment that is in dynamic equilibrium with the climatic conditions of a given region [16–18]. Saito and Matsuyama [49] and Chen et al. [17] observed that landforms in regions with high MAP are resistant to high rainfall amounts that may possibly initiate mass movements and are hence tolerant of extreme weather conditions. Similarly, Giannecchini et al. [16] noted that the critical rainfall amount for triggering landslides increases with MAP. In this study, however, differences in the regression lines for the analyzed percentiles (especially the higher percentiles) of I-D conditions (Figure 4) did not correspond well with the differences in the mean values of MAP for the three geological conditions considered (Figure 7). Furthermore, no statistically significant difference was detected in the mean values of MAP among the groups ($p = 0.531$; Figure 7). Therefore, such differences in I-D plots (Figure 4) can be attributed to geological conditions, although the regional I-D conditions reflect the various meteorological and topographical conditions of a given region [18]. This is also partially supported by Figure 6d, which shows that the mean value of I_{MAP} was significantly lower for SR terrains than for GN and GR terrains. We conclude that SR terrains have lower critical rainfall intensities than GN and GR terrains because of their relatively low soil permeability [2,5].

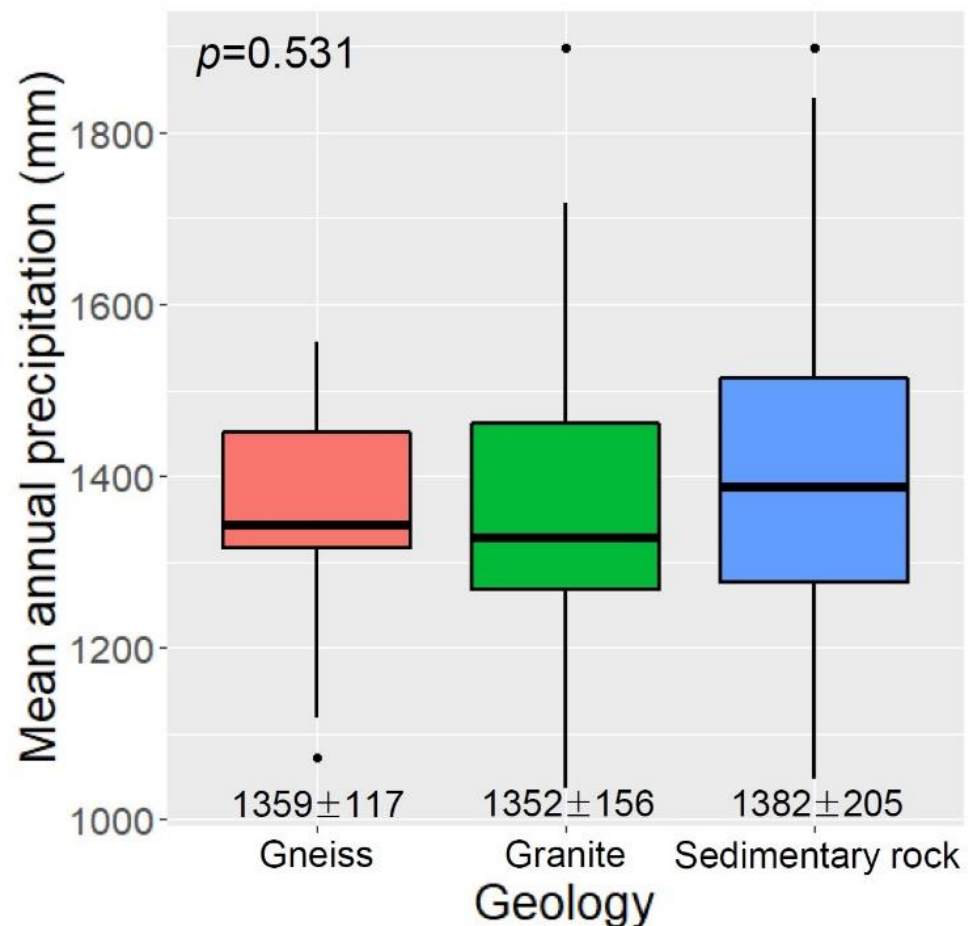


Figure 7. Boxplots of the mean annual rainfall for each geological condition. The black dots represent outliers and values below each box indicate the mean \pm standard deviation.

Percentiles are regarded as exceedance probabilities for landslide-triggering rainfall conditions [50]; therefore, they can be used to establish a landslide early warning system. For example, Piciullo et al. [50] suggested warning levels for rainfall-induced landslides based on a combination of several thresholds at different percentiles (i.e., exceedance probabilities) for cumulative rainfall–duration relationships. Our findings suggest that I-D

thresholds and rainfall amounts corresponding to the exceedance probabilities of landslide occurrences vary depending on regional geological conditions (Figure 4, Tables 1 and 2), indicating that even for the same rainfall conditions, the exceedance probability of landslide occurrence differs depending on geological conditions and is relatively high (i.e., more likely) for SR terrain than for GN and GR terrains. This finding confirms the relation of geological conditions to the I-D conditions of landslide-triggering rainfall. Furthermore, the results indicate that if the I-D conditions and thresholds for the entire country, which largely reflect the characteristics of GN and GR terrains, are employed in South Korea's landslide warning and evacuation system, false alarms could occur in SR regions.

The one-way ANOVA results reveal the differences in rainfall parameters between the SR and two other geological conditions considered, indicating that SR terrain is more susceptible to rainfall-induced landslides (Figures 5b and 6). These findings are consistent with those of Kim et al. [21], who found that the cumulative rainfall amount that triggered landslides in SR terrain was a third of that in GN terrain and half of that in GR terrains. Park et al. [51] demonstrated that soil erosion potential was much higher for SR terrain ($6.4 \text{ MT ha}^{-1} \text{ yr}^{-1}$) than for metamorphic ($5.5 \text{ MT ha}^{-1} \text{ yr}^{-1}$) and igneous ($4.3 \text{ MT ha}^{-1} \text{ yr}^{-1}$) terrains using the universal soil loss equation (USLE); they also mentioned the influence of the soil texture of parent materials. Kim and Song [5] confirmed that the rainfall intensity that caused landslides was lower in SR terrain than that in either GN or GR terrain. Igwe [6] reported that slopes in SR terrain were more susceptible to landslides than those in metamorphic areas.

Overall, these previous studies, as well as the present study, suggest that hillslopes in SR terrains are more susceptible to rainfall erosion and therefore exhibit higher landslide activity than those in GN and GR terrains. This may be strongly related to soil properties associated with weathering of parent rocks [5,51]. According to Jeong et al. [52], no significant differences were found in the physicochemical properties of soils originated from igneous and metamorphic rocks, whereas the properties of soil originating from SR are different from soils originating from igneous and metamorphic rocks. Several studies [5,35] have also shown that the geotechnical properties of soil that originated from SR are notably different from those of soil that originated from GN and GR, whereas those of soils from GN and GR are quite similar (Table 3). Thus, no significant differences existed in the mean values of rainfall parameters between GN and GR except for I_{0i} (Figures 5 and 6). Additionally, SR soil has a relatively fine-grained texture compared to igneous and metamorphic rocks [51,52]. According to Kim and Song [5], SR soil has lower values of dry unit weight, porosity, and permeability than soils from GN and GR, indicating soil impermeability (Table 3). Therefore, landslides could occur in impermeable SR hillslopes with smaller amount of rainfall and lower critical rainfall intensities than those required on permeable GN and GR hillslopes (Figures 4, 5b, and 6), as shown by Matsushi and Matsukura [14]. Moreover, soils that originate from SR have a high content of clay minerals, including particularly montmorillonite with a very high swelling potential, relative to soils from GN and GR [28]. Ohlmacher [1] showed that the plasticity index of montmorillonite is higher than that of illite, kaolinite, or chlorite for the same liquid limit. Underwood [53] noted that shales containing montmorillonite and illite are more prone to landslides than those that do not. The structure of mudstone, which is derived from SR, can easily be disrupted by water infiltration due to well-developed stratification, and hence, the hillslopes in such areas have relatively high landslide susceptibility [54]. Jun et al. [35] demonstrated that the content of silt and clay is approximately 1.8–1.9 times higher and the water content is approximately 1.3–1.4 times higher in soils derived from SR (36 sites) than in soils derived from GN (more than 156 sites) and GR (more than 500 sites) (Table 3). Gang and Jung [55] found that montmorillonite had the highest swelling ratio (approximately 152.6%) of four representative clay minerals (i.e., kaolinite, montmorillonite, illite, and bentonite) in distilled water. These observations suggest that hillslopes in SR terrains tend to collapse easily, even under low rainfall conditions [5,21,28].

Table 3. Geotechnical properties of the soil at different geological conditions in South Korea.

	GN (No. of Sites)	GR (No. of Sites)	SR (No. of Sites)	Source
Dry unit weight (g/cm ³)	1.28 (10)	1.30 (10)	1.12 (10)	Kim and Song [5]; Landslide sites
Porosity (%)	79.79 (10)	80.11 (10)	76.16 (10)	
Coefficient of permeability (cm/s)	0.00543 (10)	0.006 (10)	0.00478 (10)	
Silt and clay (%)	5.45 (156)	5.63 (500)	10.32 (36)	Jun et al. [35]; Non-landslide sites
Water content (%)	21.65 (183)	19.53 (500)	27.45 (36)	

GN: gneiss, GR: granite, and SR: sedimentary rock.

5. Conclusions

Using geological classification and hourly rainfall data for 476 landslides that occurred in Korea between 1963 and 2018, we analyzed the differences in I-D conditions and rainfall parameters for three different geological conditions using quantile regression and one-way ANOVA analyses, respectively. For quantile regression analyses of I-D and I_{MAP} -D conditions, we found that the regression lines for SR were lower after $D = 16$ h and $D = 10$ h, respectively, for the 2nd percentile and were consistently lower for both the 50th and 90th percentiles than those for GN and GR, showing that the higher the percentile is, the larger the differences are. These findings indicate that the exceedance probability of landslide occurrence varies depending on the geological conditions of a region, even under the same rainfall conditions, and is higher for impermeable SR slopes than for permeable GN and GR slopes. In addition, the results of one-way ANOVA analyses showed that the mean values of ECR, I , I_{oi} , I_{MAP} , and D/T_e were significantly lower for SR slopes than for GN and GR slopes. These results also indicate that SR slopes are more susceptible to rainfall-induced landslides than GN and GR slopes are.

Although this study relied on a statistical approach, the results clearly reveal the influence of geological conditions on I-D as well as the significant differences in the characteristics of landslide-triggering rainfall for different geological conditions (i.e., sedimentary rock vs. gneiss and granite). These findings will be very important in the development of landslide prediction and warning systems. Our findings suggest the need to consider geological conditions, particularly the relatively high susceptibility of SR to rainfall-induced landslides, in establishing rainfall information-based landslide warning criteria for South Korea, which is characterized by varied lithology. We expect our findings to contribute to future work involving landslide susceptibility and probability assessment in relation to geological conditions. In the future, the results of this study should be evaluated further by considering the aspects of soil mechanics and hydrogeology determined from in situ observations.

Author Contributions: Analysis and investigation, S.-J.J. and J.L.; resources and data curation, Y.-C.C. and S.K.; writing—original draft preparation, J.-U.L.; writing—review and editing, M.K. and S.K.; supervision, S.K. All authors have read and agreed to the published version of the manuscript.

Funding: This research was supported by the Korea Ministry of Environment as “The SS (Surface Soil Conservation and Management) Projects; 2019002830002”. This study was also supported by a 2019 Research Grant from Kangwon National University.

Institutional Review Board Statement: Not applicable.

Informed Consent Statement: Not applicable.

Data Availability Statement: Not applicable.

Conflicts of Interest: The authors declare no conflict of interest.

References

1. Ohlmacher, G.C. The relationship between geology and landslide hazards at Atchison, Kansas and vicinity. *Curr. Res. Earth Sci.* **2000**, *244*, 1–16. [[CrossRef](#)]
2. Kim, K.S. Analysis of soil characteristics and its relationship according to the geological condition in natural slopes of the landslide area. *J. Eng. Geol.* **2007**, *17*, 205–215. (In Korean with English Abstract)
3. Kim, W.Y.; Chae, B.G. Characteristics of rainfall, geology and failure geometry of the landslide areas on natural terrains, Korea. *J. Eng. Geol.* **2009**, *19*, 331–344. (In Korean with English Abstract)
4. Cevasco, A.; Pepe, G.; Brandolini, P. The influences of geological and land use settings on shallow landslides triggered by an intense rainfall event in a coastal terraced environment. *Bull. Eng. Geol. Environ.* **2014**, *73*, 859–875. [[CrossRef](#)]
5. Kim, K.S.; Song, Y.S. Geometrical and geotechnical characteristics of landslides in Korea under various geological conditions. *J. Mt. Sci.* **2015**, *12*, 1267–1280. [[CrossRef](#)]
6. Igwe, O. The geotechnical characteristics of landslides on the sedimentary and metamorphic terrains of South-East Nigeria, West Africa. *Geoenviron. Disasters* **2015**, *2*, 1. [[CrossRef](#)]
7. Bartelletti, C.; Giannecchini, R.; D'Amato Avanzi, G.; Galanti, Y.; Mazzali, A. The influence of geological–morphological and land use settings on shallow landslides in the Pogliaschina T. basin (northern Apennines, Italy). *J. Maps* **2017**, *13*, 142–152. [[CrossRef](#)]
8. Caine, N. The rainfall intensity-duration control of shallow landslides and debris flows. *Geogr. Ann. Ser. A* **1980**, *62*, 23–27.
9. Guzzetti, F.; Peruccacci, S.; Rossi, M.; Stark, C.P. The rainfall intensity-duration control of shallow landslides and debris flows: An update. *Landslides* **2008**, *5*, 3–17. [[CrossRef](#)]
10. Aleotti, P. A warning system for rainfall-induced shallow failures. *Eng. Geol.* **2004**, *73*, 247–265. [[CrossRef](#)]
11. Guzzetti, F.; Peruccacci, S.; Rossi, M.; Stark, C.P. Rainfall thresholds for the initiation of landslides in central and southern Europe. *Meteorol. Atmos. Phys.* **2007**, *98*, 239–267. [[CrossRef](#)]
12. Abraham, M.T.; Satyam, N.; Rosi, A.; Pradhan, B.; Segoni, S. The selection of rain gauges and rainfall parameters in estimating intensity-duration thresholds for landslide occurrence: Case study from Wayanad (India). *Water* **2020**, *12*, 1000. [[CrossRef](#)]
13. Cannon, S.; Gartner, J.; Wilson, R.; Bowers, J.; Laber, J. Storm rainfall conditions for floods and debris flows from recently burned areas in southwestern Colorado and southern California. *Geomorphology* **2008**, *96*, 250–269. [[CrossRef](#)]
14. Matsushi, T.; Matsukura, Y. Rainfall thresholds for shallow landsliding derived from pressure-head monitoring: Cases with permeable and impermeable bedrocks in Boso Peninsula, Japan. *Earth Surf. Process. Landf.* **2007**, *32*, 1308–1322. [[CrossRef](#)]
15. Saito, H.; Nakayama, D.; Matsuyama, H. Relationship between the initiation of a shallow landslide and rainfall intensity-duration thresholds in Japan. *Geomorphology* **2010**, *118*, 167–175. [[CrossRef](#)]
16. Giannecchini, R.; Galanti, Y.; D'Amato Avanzi, G. Critical rainfall thresholds for triggering shallow landslides in the Serchio River Valley (Tuscany, Italy). *Nat. Hazards Earth Syst. Sci.* **2012**, *12*, 829–842. [[CrossRef](#)]
17. Chen, C.W.; Saito, H.; Oguchi, T. Rainfall intensity–duration conditions for mass movements in Taiwan. *Prog. Earth Planet. Sci.* **2015**, *2*, 14. [[CrossRef](#)]
18. Kim, S.W.; Chun, K.W.; Kim, M.; Catani, F.; Choi, B.; Seo, J.I. Effect of antecedent rainfall conditions and their variations on shallow landslide-triggering rainfall thresholds in South Korea. *Landslides* **2021**, *18*, 569–582. [[CrossRef](#)]
19. Sidle, R.C.; Ochiai, H. *Landslides: Processes, Prediction, and Land Use*; American Geophysical Union: Washington, DC, USA, 2006.
20. Saito, H.; Murakami, W.; Daimaru, H.; Oguchi, T. Effect of forest clear-cutting on landslide occurrences: Analysis of rainfall thresholds at Mt. Ichifusa, Japan. *Geomorphology* **2017**, *276*, 1–7. [[CrossRef](#)]
21. Kim, K.S.; Song, Y.S.; Cho, Y.C.; Kim, W.Y.; Jeong, G.C. Characteristics of rainfall and landslides according to the geological condition. *J. Eng. Geol.* **2006**, *16*, 201–214. (In Korean with English Abstract)
22. Peruccacci, S.; Brunetti, M.T.; Luciani, S.; Vennari, C.; Guzzetti, F. Lithological and seasonal control on rainfall thresholds for the possible initiation of landslides in central Italy. *Geomorphology* **2012**, *139–140*, 79–90. [[CrossRef](#)]
23. Brand, E.W.; Premchitt, J.; Phillipson, H.B. Relationship between rainfall and landslides in Hong Kong. In Proceedings of the 4th International Symposium on Landslides, Toronto, ON, Canada, 16–21 September 1984; pp. 377–384.
24. Wieczorek, G.F. Landslide triggering mechanisms. In *Landslides: Investigation and Mitigation*; Turner, A.K., Schuster, R.L., Eds.; Transportation Research Board, National Research Council: Washington, DC, USA, 1996; pp. 76–90.
25. Guzzetti, F.; Cardinali, M.; Reichenbach, P. The influence of structural setting and lithology on landslide type and pattern. *Environ. Eng. Geosci.* **1996**, *2*, 531–555. [[CrossRef](#)]
26. Kim, W.Y.; Kim, K.S.; Chae, B.G.; Cho, Y.C. Case study of landslide types in Korea. *J. Eng. Geol.* **2000**, *10*, 18–35. (In Korean with English Abstract)
27. Kim, K.S.; Lee, M.S.; Cho, Y.C.; Che, B.G.; Lee, C.O. Engineering characteristics of soil slopes dependent on geology: Hwangryeong Mt. district, Busan. *J. Eng. Geol.* **2004**, *14*, 487–498. (In Korean with English Abstract)
28. Kim, K.S.; Choo, C.O.; Booh, S.A.; Jeong, G.C. Importance of microtextural and geochemical characterizations of soils on landslide sites. *J. Eng. Geol.* **2005**, *15*, 447–462. (In Korean with English Abstract)
29. Kim, S.W.; Chun, K.W.; Otsuki, K.; Shinohara, Y.; Kim, M.I.; Kim, M.S.; Lee, D.K.; Seo, J.I.; Choi, B. Heavy rain types for triggering shallow landslides in South Korea. *J. Fac. Agric. Kyushu Univ.* **2015**, *60*, 243–249. [[CrossRef](#)]
30. Korea Meteorological Administration. *The Climate Atlas of Korea*; Korea Meteorological Administration: Seoul, Korea, 2012. (In Korean)

31. Korea Research Institute for Human Settlements. *Policy Measurement for the Efficient Management of Forest Land*; Korea Forest Service: Daejeon, Korean, 2008. (In Korean)
32. Kim, S.W.; Chun, K.W.; Kim, K.N.; Kim, M.S.; Kim, M.S.; Lee, S.H.; Seo, J.I. Significance and future direction for designation and management of landslide-prone zones. *J. Forest Sci.* **2013**, *29*, 237–248. (In Korean with English abstract)
33. National Geographic Information Institute. *The Geography of Korea*; National Geographic Information Institute: Suwon-si, Korea, 2010.
34. Lim, H.S. Cretaceous sedimentary basins and volcanic activity in Korea. *J. Geol. Soc. Korea* **2019**, *55*, 493–494. (In Korean with English abstract) [[CrossRef](#)]
35. Jun, D.C.; Song, Y.S.; Han, S.I. Proposal of models to estimate the coefficient of permeability of soils on the natural terrain considering geological conditions. *J. Eng. Geol.* **2010**, *20*, 35–45. (In Korean with English abstract)
36. National Geographic Information Institute. *The National Atlas of Korea II*; National Geographic Information Institute: Suwon-si, Korea, 2016.
37. Kim, S.; Oh, W.; Lee, S. Analysis on the density of the weather station over South Korea. *Geogr. J. Korea* **2013**, *47*, 47–59. (In Korean with English abstract)
38. World Meteorological Organization. *The Role of Climatological Normal in a Changing Climate*; WMO-TD No. 1377; World Meteorological Organization: Geneva, Switzerland, 2007.
39. Korea Meteorological Administration. *Climatological Normals of Korea (1961–1990)*; Korea Meteorological Administration: Seoul, Korea, 1991. (In Korean)
40. Korea Meteorological Administration. *Climatological Normals of Korea (1971–2000)*; Korea Meteorological Administration: Seoul, Korea, 2001. (In Korean)
41. Rosi, A.; Segoni, S.; Catani, F.; Casagli, N. Statistical and environmental analyses for the definition of a regional rainfall threshold system for landslide triggering in Tuscany (Italy). *J. Geogr. Sci.* **2012**, *22*, 617–629. [[CrossRef](#)]
42. Peres, D.J.; Cancelliere, A. Derivation and evaluation of landslide-triggering thresholds by a Monte Carlo approach. *Hydrol. Earth Syst. Sci.* **2014**, *18*, 4913–4931. [[CrossRef](#)]
43. Segoni, S.; Battistini, A.; Rossi, G.; Rosi, A.; Lagomarsino, D.; Catani, F.; Moretti, S.; Casagli, N. Technical note: An operational landslide early warning system at regional scale based on space–time-variable rainfall thresholds. *Nat. Hazards Earth Syst. Sci.* **2015**, *15*, 853–861. [[CrossRef](#)]
44. Ministry of Land, Infrastructure and Transport. *Development of Warning and Evacuation System for Sediment Disaster in Developing Countries*; Ministry of Land, Infrastructure and Transport: Tokyo, Japan, 2004.
45. National Institute for Disaster Prevention. *A Study on the Monitoring and Detection of Slope Failure (II): Focusing on the Application of Rainfall Data*; Ministry of Government Administration and Home Affairs: Seoul, Korea, 2005. (In Korean)
46. Park, J.Y.; Lee, S.R.; Lee, D.H.; Kim, Y.T.; Oh, S.; Park, H.J. Development of continuous rainfall-based citywide landslide early warning model. *J. Korean Soc. Hazard. Mitig.* **2018**, *18*, 99–111. (In Korean with English abstract) [[CrossRef](#)]
47. Koener, R.W. Quantile Regression in R: A Vignette. 2009. Available online: <http://www.cran.r-project.org/web/packages/quantreg/vignettes/rq.pdf> (accessed on 15 April 2019).
48. Jakob, M.; Weatherly, H. A hydroclimatic threshold for landslide initiation on the North Shore Mountains of Vancouver, British Columbia. *Geomorphology* **2003**, *54*, 137–156. [[CrossRef](#)]
49. Saito, H.; Matsuyama, H. Catastrophic landslide disasters triggered by record-breaking rainfall in Japan: Their accurate detection with normalized soil water index in the Kii Peninsula for the year 2011. *SOLA* **2012**, *8*, 81–84. [[CrossRef](#)]
50. Piciullo, L.; Gariano, S.L.; Melillo, M.; Brunetti, M.T.; Peruccacci, S.; Guzzetti, F.; Calvello, M. Definition and performance of a threshold-based regional early warning model for rainfall-induced landslides. *Landslides* **2017**, *14*, 995–1008. [[CrossRef](#)]
51. Park, C.W.; Sonn, Y.K.; Hyun, B.K.; Song, K.C.; Chun, H.C.; Cho, H.J.; Moon, Y.H.; Yun, S.G. Soil erosion risk assessment by soil characteristics and landuse in the upper Nakdong River basin. *Korean J. Soil Sci. Fertil.* **2012**, *45*, 890–896. (In Korean with English Abstract) [[CrossRef](#)]
52. Jeong, J.; Kim, C.; Goo, K.; Lee, C.; Won, H.; Byun, J. Physico-chemical properties of Korean forest soils by parent rocks. *J. Korean For. Soc.* **2003**, *92*, 254–262. (In Korean with English abstract)
53. Underwood, L.B. Classification and identification of shales. *J. Soil. Mech. Found. Div. Proc. Am. Soc. Civil. Eng.* **1967**, *93*, 97–116. [[CrossRef](#)]
54. Korea Institute of Geoscience and Mineral Resources. *Study on Landslide Hazard Prediction*; Report of Ministry of Science and Technology No. KR-03-(T)-03; Korea Institute of Geoscience and Mineral Resources: Seoul, Korea, 2003.
55. Gang, S.G.; Jung, J. Swelling characteristics of clay minerals according to the ionic strength in pore water. *J. Korean Soc. Hazard. Mitig.* **2021**, *21*, 201–207. (In Korean with English Abstract) [[CrossRef](#)]